Capsular Biofilm Formation at the Interface of Textured Expanders and Human Acellular Dermal Matrix: A Comparative Scanning Electron Microscopy Study

Michel A. Danino, M.D., Ph.D.
Johnny I. Efanov, M.D.
Georges Dimitropoulos, M.D.
Maxim Moreau, Ph.D.
Charles Maalouf, M.D.
Monica Nelea, Ph.D.
Ali Izadpanah, M.D., M.Sc.
Jean-Philippe Giot, M.D.

Montreal, Quebec, Canada

Background: Despite benefits in reducing capsular contractures, textured implants have been associated with significant pitfalls, such a propensity for biofilm formation. Few studies have investigated whether the use of acellular dermal matrix on textured implants produces similar findings. This study aims to characterize biofilm formation at the capsular–acellular dermal matrix interface with scanning electron microscopy.

Methods: The authors performed a prospective observational pilot study in patients undergoing two-stage expander-to-permanent implant exchange. Patients were inflated with Biocell or Siltex expanders, and specimens from the capsular-pectoralis interface and capsular–acellular dermal matrix interface were obtained and examined under scanning electron microscopy for capsular ingrowth and biofilm formation using the Van Herdeen Biofilm Grading System and the Biofilm Thickness Grading Scale.

Results: Nine patients including 14 breasts (28 capsular samples in total) were examined. Thick biofilm formation was observed in all specimens from the capsular–acellular dermal matrix interface with Biocell and 25 percent of capsule-pectoralis interface, whereas no biofilm formation was found in Siltex implants. For Biocell implants, a significant difference in biofilm coverage between the upper and lower poles was observed using the Van Herdeen Biofilm Grading System ($p = 0.0028$) and the Biofilm Thickness Grading Scale ($p = 0.0161$).

Conclusions: Biocell implants produce a significant rate of biofilm formation over acellular dermal matrix–covered capsules, which is not present in the muscular region or in Siltex implants. Further randomized controlled trials will further elucidate the clinical impact of using acellular dermal matrices with macrotextured implants. (*Plast. Reconstr. Surg.* 141: 919, 2018.)

CLINICAL QUESTION/LEVEL OF EVIDENCE: Therapeutic, IV.

Macrotexturing of breast implants was originally developed with the purpose of stabilizing and minimizing rotation of prostheses within the breast pocket.[1–3] By minimizing movement of the implant, it was observed that macrotextured or high-surface-area textured implants produced lower rates of capsular contracture, especially when placed submuscularly.[4,5] Other notable advantages included decreased rates of malposition, rotation, and rippling[6,7] and greater patient satisfaction,[8,9] which resulted in the era of textured implants. However, potential drawbacks limited their use in recent years, most

From the Plastic and Reconstructive Surgery Department, Notre-Dame Hospital, University of Montreal Hospital Center.
Received for publication October 3, 2017; accepted October 18, 2017.
Presented at Plastic Surgery The Meeting 2016, Annual Meeting of the American Society of Plastic Surgeons, in Los Angeles, California, September 23 through 27, 2016.

DOI: 10.1097/PRS.0000000000004216

Disclosure: *Dr. Danino is a consultant and speaker for Allergan, Inc. None of the other authors has any commercial associations or financial interests to declare with respect to any of the information or products presented in this article. Operational study costs were supported in part by an Allergan, Inc., industry research grant.*

notably a propensity for double-capsule formation,[10,11] late seromas,[12,13] biofilms,[14] and an association with anaplastic large-cell lymphomas.[15,16] As a result, studies investigating microscopic pathophysiologic changes in macrotextured implants have gained in popularity, expanding our knowledge about these worrisome phenomena.

The surface morphology of macrotextured implants has been described before.[17–20] Biocell macrotextured (or high-surface-area textured) shell surfaces (Allergan, Inc., Irvine, Calif.) are produced through the "lost salt technique," in which the implant's shell is pressed against a layer of fine salt. In contrast, Siltex microtextured (or low-surface-area textured) implants (Mentor Worldwide, Santa Barbara, Calif.) are manufactured through negative contact imprinting from textured foam, a less aggressive form of texturization. Previous studies have demonstrated that capsules removed from macrotextured implants imprint the surface morphology as mirror images,[3] with a greater degree measured in Biocell than in Siltex implants. Aggressive texture adheres to periprosthetic capsules with significant grip, often necessitating forceps to peel it off intraoperatively, known as the "Velcro effect."[21]

Concurrently, acellular dermal matrix solidified its role as an effective tool to support the lower pole breast pocket after reconstruction or augmentation.[22] Histologic analyses of breast capsules in contact with acellular dermal matrices have demonstrated less inflammation and fewer myofibroblasts than non–acellular dermal matrix capsules, explaining in part the potential benefit in reducing capsular contractures as reported in the literature.[23] However, there have been no studies investigating the microscopic morphologic changes at the interface of acellular dermal matrices with macrotextured implants. The goal of this study was to evaluate the impact of acellular dermal matrix on the capsular architecture of breasts.

PATIENTS AND METHODS

A prospective observational study was developed, with recruitment of patients undergoing two-stage expander-to-permanent implant exchange for reconstruction after breast cancer surgery. To investigate microscopic changes at the interface of acellular dermal matrix and implants, only patients for whom AlloDerm (LifeCell Corp., Branchburg, N.J.) was used during the expander insertion were asked to consent for participation in the study. The research protocol was approved by our institution's review board in accordance with the Declaration of Helsinki.

All patients included in this study were operated on at the same university hospital center by one of three plastic surgeons. During the first-stage mastectomy and expander insertion, first-generation cephalosporin was administered at induction and skin preparation was performed with standard aseptic technique using a solution of chlorhexidine 4% with alcohol. Subpectoral dissection was performed using electrocautery to create the upper pole's breast pocket. The only two commercially available expanders in Canada are Biocell and Siltex, which were used alternatively. Breast expanders were inserted into the breast pocket after submersion and irrigation in bacitracin solution, exchange of surgical gloves, and addition of sterile surgical drapes. Construction of lower pole breast pockets was performed with AlloDerm attached to the inframammary fold and pectoral muscle with absorbable sutures. Two-layer skin closure was completed, with installation of Jackson-Pratt drains and sterile dressings. Intraoperative expander filling and postoperative expansion followed each surgeon's own management approach for initial filling percentage, timing of first inflation, and weekly volume expanded.

Data collection consisted of baseline patient demographics and pertinent risk factors such as chemotherapy or radiotherapy. Data pertaining to the surgical procedure included the type of mastectomy performed, implant sizes, number of drains, and occurrence of postoperative complications. Patients with postoperative infection, significant inflammation, or technical difficulty with sampling were excluded.

During the second-stage expander-to-permanent implant exchange, clinical observations of periprosthetic capsules were recorded for the appearance of a coating film, the Velcro effect, or double capsules. The appearance of biofilm was defined as reflective layers of film between the implant and the capsule. The Velcro effect was considered positive when the removal of the prosthesis from the surrounding capsule required the use of a forceps to peel it off. Double capsules corresponded to implants surrounded by two distinct capsules.

Capsular sampling consisted of two specimens from each patient measuring 1 × 1 cm. The first sample was collected from the capsular tissue taken in the upper pole adjacent to the pectoralis muscle, and the second sample was taken from the capsular tissue adjacent to the lower pole where the acellular dermal matrix was used. Tissue specimens were tagged with sutures in which the knots were applied on the capsule's surface facing the

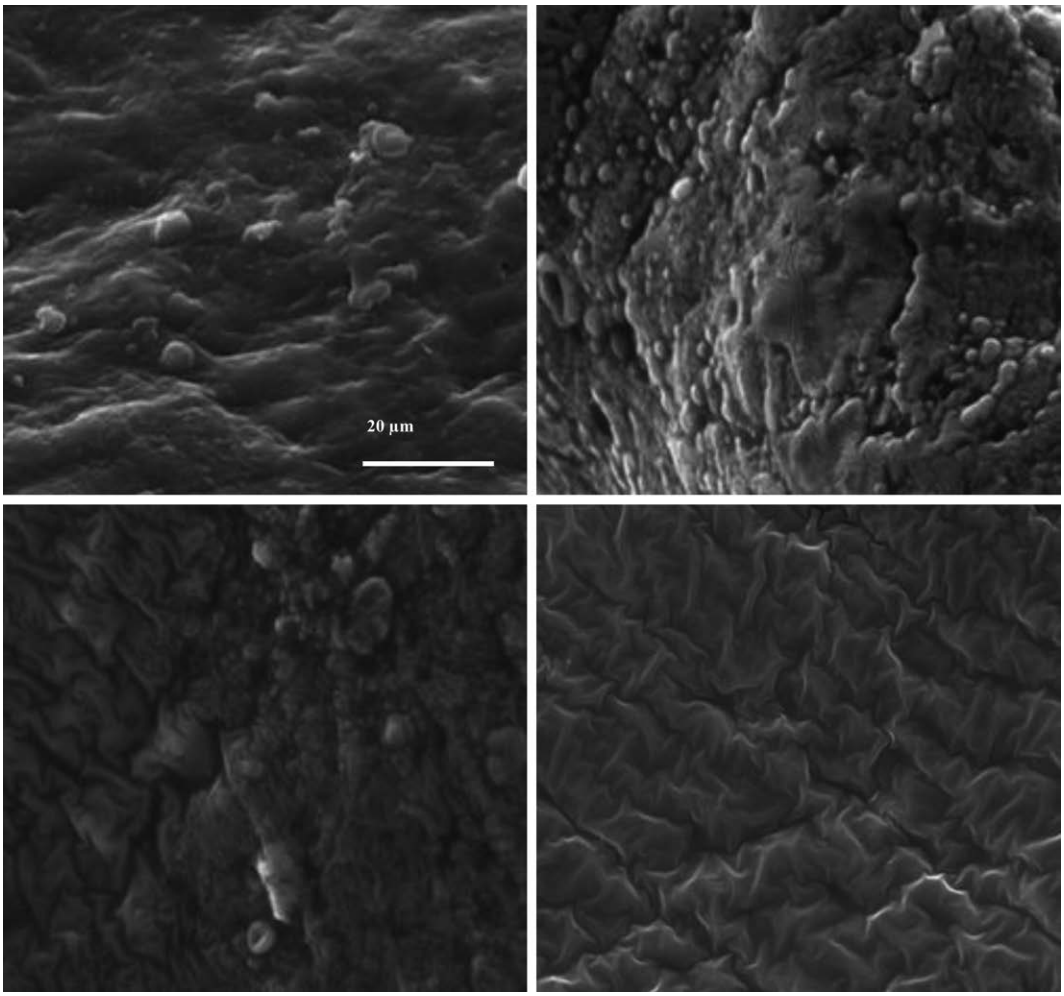

Fig. 1. Van Herdeen Biofilm Grading System used to classify specimens according to surface area of biofilm coverage on the breast implants. (*Above*, *left*) Scanning electron microscopic image of a specimen harvested on the muscular interface of a Biocell implant in patient 2 (left breast) (original magnification, × 3000). The image demonstrates a lack of biofilm coverage, with a smooth, uniform background and scarce round bacterial cells (Van Herdeen grade 0). (*Above*, *right*) Scanning electron microscopic image from a specimen harvested on the muscular interface of a Biocell implant in patient 2 (right breast) (original magnification, × 3000). The image reflects the formation of small areas of biofilm coverage with a higher proportion of underlying bacteria (Van Herdeen grade 1). (*Below*, *left*) Scanning electron microscopic image from a specimen harvested on the muscular interface of a Biocell implant in patient 4 (right breast) (original magnification, × 3000). The capsule is covered by a larger surface area of biofilm, but has yet to be completely covered (Van Herdeen grade 2). (*Below*, *right*) Scanning electron microscopic image from a specimen harvested on the acellular dermal matrix interface of a Biocell implant in patient 2 (right breast) (original magnification, × 3000). The image is typical of a large surface area covered completely with a biofilm layer, imprinting the underlying architecture of the implant (Van Herdeen grade 3). Bacteria are invisible on this interface because they are located under a complete coverage of biofilm.

expander and immediately fixed in a solution of 2% glutaraldehyde in sodium cacodylate 0.1 M buffer with a pH of 7.3. Capsular samples were stored in a refrigerator at 4°C for a minimum of 24 hours until examination under microscopy.

Samples were analyzed using the scanning electron microscopy using the ESEM Quanta FEG 200 (FEI Company, Hillsboro, Ore.) at high-vacuum (HiVac) operating mode and with energy dispersive x-ray spectroscopy. Observations were conducted under 100× to 3000× magnification. Micrographs were analyzed using XT Docu (FEI Company) and texture measurements were performed using Adobe Photoshop CS6 Extended

Table 1. Grading Systems Used for Analysis of Biofilm Coverage on Breast Implants

	Description
Van Herdeen Biofilm Grading System for surface area	
Grade 0	No biofilm coverage
Grade 1	Small area of biofilm coverage
Grade 2	Medium area of biofilm coverage
Grade 3	Large area of biofilm coverage
Biofilm Thickness Grading Scale for Thickness	
Grade 0	No biofilm
Grade 1	Thin, where extracellular matrix does not cover bacteria
Grade 2	Thick, with underlying capsular architecture still distinguishable
Grade 3	Very thick, with masking of the underlying capsular architecture

(Adobe Systems, Inc., San Jose, Calif.) with a 2 percent margin of error.

Observations were performed by an independent collaborator that was blinded to the type of implant and the interface to prevent observer bias. These images were charted to tally and objectify three parameters: (1) texture (i.e., surface relief characterization), (2) cellularity (i.e., cell count and characterization), and (3) biofilm (i.e., presence/absence, characterization), as described previously by our team.[19] More specifically for biofilm characterization, we measured the surface area involved using the Van Herdeen Biofilm Grading System[24] (Fig. 1) and the relative thickness using our in-house Biofilm Thickness Grading Scale (Table 1 and Fig. 2). Capsular specimens from the implant–acellular dermal matrix interface were compared with those taken from the implant-pectoralis interface, and a correlation between the two scales was then performed. For statistical analysis, capsular samples were divided into two groups (implant–acellular dermal matrix versus implant-pectoralis), with further subgroup analysis according to the type of expander used (Biocell versus Siltex). Paired *t* tests were performed between groups with a significance level set at a value of $p < 0.05$.

RESULTS

Analysis of outcomes included 28 capsule samples from 14 breasts in nine women (Fig. 3). Three patients underwent bilateral prophylactic nipple-sparing mastectomy for *BRCA*, two had bilateral total mastectomies for breast cancer, and four required unilateral total mastectomies. Sentinel lymph node biopsies were performed on two patients, one bilateral and one unilateral. During the first stage of total mastectomy and expander insertion, eight breasts were augmented with Allergan's Biocell and six breasts with Mentor's Siltex. The average size was 490 cc, and all procedures were performed with submuscular insertion assisted by AlloDerm (16 × 8 cm). Mean operating time was 212 minutes, including total mastectomies and expander insertion, and there was only one postoperative complication, a hematoma that required evacuation (Table 2).

Definitive expander-to-implant exchange occurred between 4 and 16 months after the first stage, depending on the surgeon's protocol for inflation and need for postoperative adjuvant treatments. At the implant-muscle interface with Biocell expansion, the Velcro effect was clinically identifiable in all eight specimens, which resulted in forceps harvesting of the capsule from the implant. When examined under electron microscopy, all eight Biocell capsules demonstrated macrotexturing ingrowth from the implant's pores. However, 25 percent of specimens ($n = 2$) presented with thick biofilm, but with capsular architecture underneath that was still distinguishable. In comparison, specimens from the implant–acellular dermal matrix interface with Biocell expansion had no clinically identifiable Velcro effect or macrotexturing ingrowth, but a rate of 100 percent ($n = 8$) for biofilm formation under electron microscopy.

For cases treated with Siltex, observations at the implant-muscle interface failed to demonstrate clinically identifiable Velcro effect and macrotexturing ingrowth of the capsule from the implant's pores. Despite few bacteria present, none of the six specimens presented with biofilm formation under electron microscopy. When samples from the implant–acellular dermal matrix interface with Siltex were examined, all specimens failed to present with Velcro effect and macrotexturing ingrowth. They also did not present with biofilm formation, which differed from findings from the Biocell group. Table 3 compares results from the Biocell and Siltex groups at the implant-muscle and implant–acellular dermal matrix interfaces.

Further evaluation of biofilm formation under electron microscopy was performed using the Van Herdeen Biofilm Grading System for surface area and the Biofilm Thickness Grading Scale described previously (Table 4). In the Biocell group, there was a statistically significant difference in the biofilm coverage as measured by the Van Herdeen Biofilm Grading System ($p = 0.0028$) and in relative thickness ($p = 0.0161$) when comparing implant-muscle and implant–acellular dermal matrix interfaces from the same breasts (Fig. 4). Biofilm thickness and coverage scales were strongly related

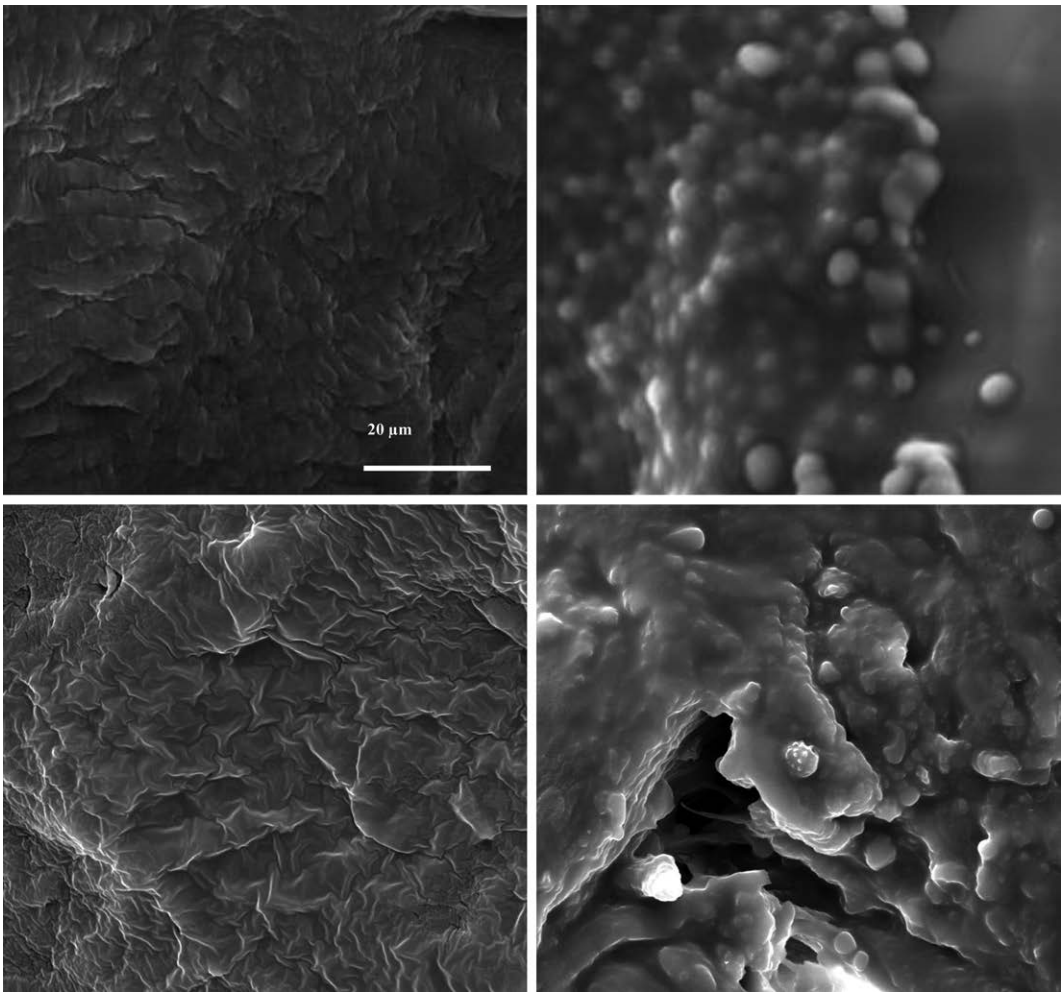

Fig. 2. Biofilm Thickness Grading Scale used to measure thickness of biofilm coverage on the breast implants. (*Above*, *left*) Scanning electron microscopic image from a specimen harvested on the muscular interface of a Biocell implant in patient 1 (right breast) (original magnification, × 3000). The image demonstrates a capsular surface with no visible biofilm (Biofilm Thickness grade 0). (*Above*, *right*) Scanning electron microscopic image from a specimen harvested on the acellular dermal matrix interface of a Biocell implant in patient 1 (right breast) (original magnification, × 3000). A thin layer of biofilm is developing on the left side of the image, but extracellular matrix has yet to cover the bacteria and form a thick biofilm (Biofilm Thickness grade 1). (*Below*, *left*) Scanning electron microscopic image from a specimen harvested on the muscular interface of a Biocell implant in patient 5 (right breast) (original magnification, × 3000). A thicker biofilm layer has developed covering the entirety of illustrated specimen, but the underlying capsular architecture is still distinguishable (Biofilm Thickness grade 2). (*Below*, *right*) Scanning electron microscopic image from a specimen harvested on the acellular dermal matrix interface of a Biocell implant in patient 5 (right breast) (original magnification, × 3000). The specimen illustrated in this image contains a very thick biofilm, with several layers of bacteria within the biofilm and masking of the underlying capsular architecture (Biofilm Thickness grade 3).

(r^2 = 0.8452, p = 0.0002), consistent with biofilm growth spreading from few cells attached to a surface (Fig. 5).

DISCUSSION

Despite long-term benefits for aesthetic outcomes and shorter time to reconstruction for two-stage procedures, acellular dermal matrix is associated with a higher rate of early complications compared with total submuscular implants, namely, for infections and seroma formation.[25,26] Previous studies have focused on patient risk factors and treatment characteristics predictive of complications,[27] but an etiologic hypothesis has

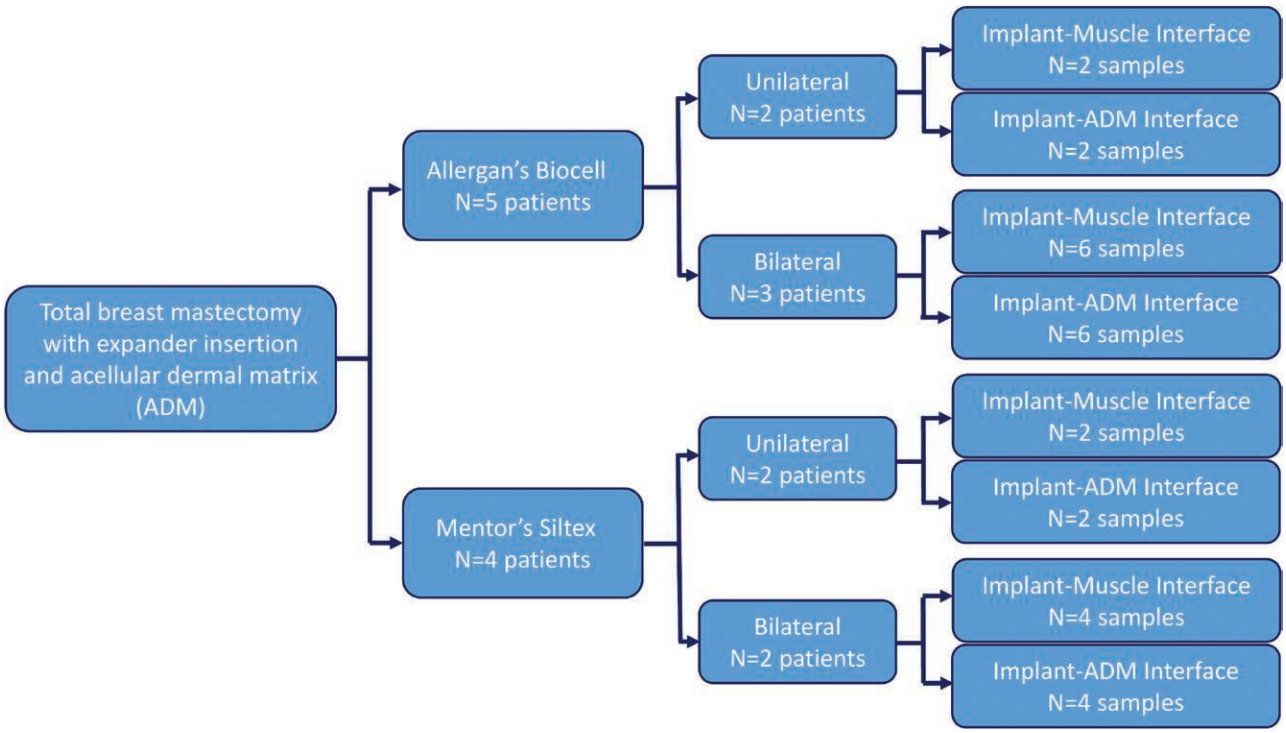

Fig. 3. Flowchart illustrating different groups of specimens harvested from the muscle or acellular dermal matrix (*ADM*) interface in Biocell and Siltex implants.

yet to be validated. Furthermore, the interaction between acellular dermal matrices and high-surface-area textured implants merits further attention in the context of recent pitfalls encountered with anatomical textured prostheses.[11,28] Our study aimed to elucidate microscopic changes occurring at the implant–acellular dermal matrix interface with the use of scanning electron microscopy, which has yet to be performed in the breast literature.

Microbial cell embedment within extracellular polymeric matrices surrounding breast

Table 2. Patient Characteristics and Operative Details of Patients Included for Capsular Analysis of Implant-Muscle and Implant–Acellular Dermal Matrix Interfaces by Scanning Electron Microscopy

Patient	Age (yr)	BMI (kg/m^2)	Active Smoker	Comorbidity	Indication for Surgery	Procedure
1	37	21	Yes	Hysterectomy	Prophylactic *BRCA*	Nipple-sparing total mastectomy
2	64	30	No	Dyslipidemia, asthma, depression	Breast cancer	Total mastectomy and sentinel lymph node dissection
3	54	20.8	No	Scoliosis, osteoporosis, asthma	Breast cancer	Total mastectomy and sentinel lymph node dissection
4	50	23.9	No	Ovarian cancer, depression	Breast cancer	Total mastectomy
5	75	20.2	No	Nil	Breast cancer	Total mastectomy
6	24	22.7	No	Nil	Breast cancer	Total mastectomy
7	70	25	No	Hypertension, dyslipidemia	Breast cancer	Total mastectomy
8	65	24.9	No	Depression	Prophylactic *BRCA*	Nipple-sparing total mastectomy
9	55	18.7	No	Nil	Prophylactic *BRCA*	Nipple-sparing total mastectomy
Average	54.89	23.02				

ADM, acellular dermal matrix; BMI, body mass index; JP, Jackson-Pratt.

implants is often referred to as a biofilm. Eliminating biofilm layers is often unattainable, because bacteria undergo phenotypic changes allowing them to combat host defenses and antibiotics.[29] There is compelling evidence that, although not proved to be the cause, biofilms are associated with persistent infections,[30] late seromas,[31] capsular contractures,[32] and potentially anaplastic large-cell lymphoma.[28] More specifically for lower pole reconstruction with acellular dermal matrices, biofilm formation can occur as demonstrated by Nyame et al. with an assay that accurately quantified bacterial adherence in an in vitro setting.[33] We developed an in vivo model investigating whether capsules underlined by acellular dermal matrices produce a higher rate of microbial colonization than surrounding normal breast pocket.

When comparing capsular interfaces between regions abutting the pectoralis muscle or the acellular dermal matrix support, we noticed a significant increase in thick biofilm formation underlying the acellular dermal matrix for macrotextured Biocell implants. Indeed, we identified that all eight analyzed samples differed when matched across acellular dermal matrix and muscular interfaces in terms of the biofilm surface area and relative thickness, which was statistically significant ($p = 0.0028$ and $p = 0.0161$, respectively). The microstructural architecture of the acellular dermal matrix does not provide capsular ingrowth from the high-surface-area texture of the implant of Biocell. This results in dead spaces prone to microbial proliferation and subsequent biofilm formation, which was mostly observed in areas with a lack of the Velcro effect and capsular ingrowth. The presence of capsular ingrowth into pores of the Biocell implant at the pectoralis interface, and the consequent Velcro effect, could explain the lower rate of biofilm formation in the upper section. Another plausible hypothesis could reside in mechanical forces from gravitational pull and from the higher volume present in the lower pole for anatomical Biocell implants, producing mechanical micromovements and sheer stress over the acellular dermal matrix regions to a greater degree than it would in the upper poles.[10] Other theories to consider would be higher contamination loads from the acellular dermal matrix during operative insertion and extensive manipulation or closer proximity to surgical scars and surrounding skin flora. However, the latter explanation would have resulted in biofilm formation for Siltex patients as well.

Another interesting finding was that, despite higher rates of biofilm formation over the acellular dermal matrix–covered capsule, patients did not present with an increased incidence of clinical capsular contractures. Previous studies have demonstrated a correlation between biofilm formation and capsular contracture; however, none of them investigated this relationship in conjunction with the use of acellular dermal matrices.[32] Whether a regulatory effect of the matrix on myofibroblastic contraction could explain this phenomenon or whether the muscular upper pole being free of

Side	Implant Type	Expander Size (cc)	ADM Size (cm)	JP Drains	Blood Loss (cc)	Operating Time (min)	Complications
Bilateral	Allergan Biocell	410	16 × 8	2	75	180	Nil
Bilateral	Allergan Biocell	600	16 × 8	4	0	300	Nil
Unilateral (right)	Mentor Siltex	350	16 × 6	2	100	115	Immediate postoperative hematoma evacuated
Unilateral (right)	Allergan Biocell	400	16 × 8	1	0	250	Nil
Unilateral (right)	Allergan Biocell	400	16 × 8	2	50	195	Nil
Bilateral	Allergan Biocell	500	16 × 8	4	100	300	Nil
Unilateral (right)	Mentor Siltex	650	16 × 6	1	0	150	Nil
Bilateral	Mentor Siltex	550	16 × 8	4	0	200	Nil
Bilateral	Mentor Siltex	550	16 × 6	2	75	215	Nil
		490		2.44	44.44	211.67	

Table 3. Clinical and Microscopic Findings When Comparing Biocell and Siltex at Different Capsular Interfaces

Patient	Time between Stages (mo)	Side	Velcro Effect	Capsular Ingrowth	Thick Biofilm Formation
Biocell					
Implant-muscle interface					
1	16	Right	+	+	−
		Left	+	+	−
2	16	Right	+	+	−
		Left	+	+	−
4	9	Right	+	+	+
5	8	Right	+	+	+
6	9	Right	+	+	−
		Left	+	+	−
Implant-ADM interface					
1	16	Right	−	−	+
		Left	−	−	+
2	16	Right	−	−	+
		Left	−	−	+
4	9	Right	−	−	+
5	8	Right	−	−	+
6	9	Right	−	−	+
		Left	−	−	+
Siltex					
Implant-muscle interface					
3	5	Right	−	−	−
7	8	Right	−	−	−
8	5	Right	−	−	−
		Left	−	−	−
9	4	Right	−	−	−
		Left	−	−	−
3	5	Right	−	−	−
Implant-ADM interface					
7	8	Right	−	−	−
8	5	Right	−	−	−
		Left	−	−	−
9	4	Right	−	−	−
		Left	−	−	−

+, with; −, without; ADM, acellular dermal matrix.

Table 4. Van Herdeen Biofilm Grading System for Surface Area and Biofilm Thickness Grading Scale for Relative Thickness at Different Interfaces for Biocell Implants

Patient and Side	Van Herdeen Grade on ADM	Van Herdeen Grade on Muscle	Biofilm Thickness Grade on ADM	Biofilm Thickness Grade on Muscle
1				
Right	2	0	1	0
Left	2	0	1	0
2				
Right	3	1	3	1
Left	1	0	2	1
4				
Right	3	2	3	2
5				
Right	2	0	3	2
6				
Right	3	0	3	0
Left	3	0	3	0

ADM, acellular dermal matrix.

biofilm plays a protective role are hypotheses that merit further investigation.

This study is also the first to compare Biocell and Siltex implants used in conjunction with acellular dermal matrices in relation to biofilm formation. Observations in Siltex samples taken from the acellular dermal matrix side failed to demonstrate microbial proliferation in a slim layer. Mentor's textured implants do not present significant microscopic depressions in their architecture to the same extent as Biocell does with their lost-salt technique. As such, dead space for bacterial proliferation is reduced, which could explain the lower rate of biofilms.

To examine the interaction between acellular dermal matrices and macrotextured implants, we developed a model using two-stage expander-to–permanent implant exchange for reconstruction after breast cancer. Some might argue that findings from this type of methodology would not apply to long-term definitive implants. Although imperfect in extrapolating results from this patient population to aesthetic augmentations, we believe this model constitutes the closest estimation of microscopic pathophysiologic changes around prostheses in an in vivo setting. Considering that patients included in this study had variable lengths between expander insertion and definitive implant placement (i.e., 4 to 16 months), it is reasonable to assume that biofilm formation at the implant–acellular dermal matrix interface occurs relatively early and persists in the long term. Had this study been performed on definitive implants with longer follow-up periods, biofilm formation on the acellular dermal matrix side should have followed the same trend. It is difficult to presume whether bacterial proliferation would have spread to the implant-muscular interface, a question that merits further prospective studies performed on implant–acellular dermal matrix revisions for capsular contractures.

If further studies performed on different models demonstrate similar rates of biofilm formation when acellular dermal matrix is used, it could be beneficial to revisit implant choice selection or to develop new manufacturing techniques to address this problem. For instance, it would be interesting to determine whether an anatomical implant with a macrotextured layer in the upper pole and a smooth surface at the lower pole abutting the acellular dermal matrix would provoke similar findings.

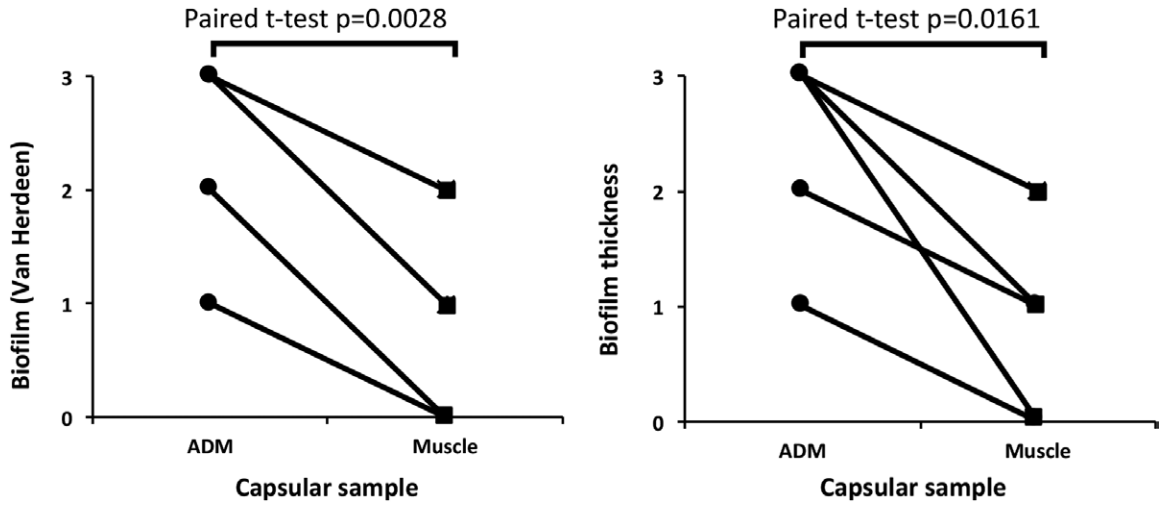

Fig. 4. Differences in surface area involvement (Van Herdeen Biofilm Grading System) and biofilm thickness under scanning electron microscopy at the acellular dermal matrix (*ADM*) and muscular interfaces for Biocell implants.

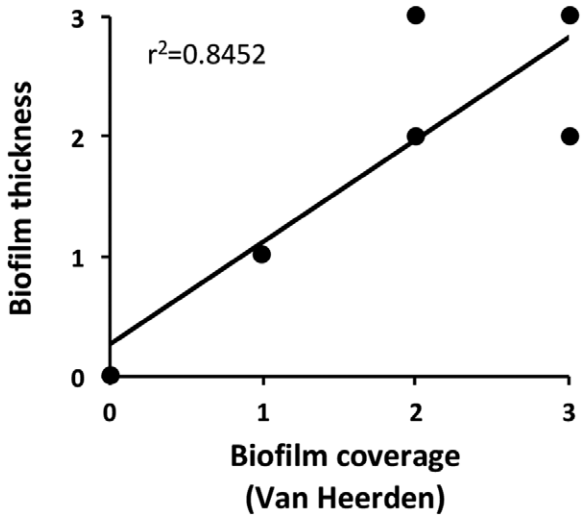

Fig. 5. Correlation between surface area involvement and biofilm thickness measured on scanning electron microscopy for Biocell implants.

This study is limited in its prospective design, wherein patients were not randomized to the Biocell or Siltex group and controlled for duration of expansion. Some studies have demonstrated that variations in expansion protocols could lead to observable modifications in capsular architecture,[34] a variable that should be accounted for in further studies. Furthermore, Biocell expanders were kept in for longer periods compared with Siltex in this patient population. However, patients 4 and 5, who had a second-stage procedure at half the time of patients 1 and 2, demonstrates that biofilm formation had ample time to occur in a shorter timeframe nonetheless. Finally, our study suffers from a limited number of patients, which did not allow analysis of patient characteristics and operative variables as confounding factors. To the best of our knowledge, this remains the largest study to date investigating the interaction of acellular dermal matrices with macrotextured implants by scanning electron microscopy.

CONCLUSIONS

Acellular dermal matrix will continue to occupy an important role in lower breast support for breast reconstruction and augmentation. Because use of macrotextured implants is currently being revisited because of significant health risks, understanding the pathophysiologic changes occurring at the implant–acellular dermal matrix interface is fundamental. Our findings demonstrate that Biocell implants produce a significant rate of biofilm formation over the acellular dermal matrix–covered capsule that is not present over the muscular region and in Siltex implants. Further randomized controlled trials will further elucidate the clinical impact of using acellular dermal matrices with macrotextured prostheses.

Michel A. Danino, M.D., Ph.D.
Notre-Dame Hospital
University of Montreal Hospital Center
1560 Rue Sherbrooke Est
Montreal, Quebec H2L 4M1, Canada
daninoalain@gmail.com

ACKNOWLEDGMENT

Operational study costs were supported in part by an Allergan, Inc., industry research grant.

REFERENCES

1. Steiert AE, Boyce M, Sorg H. Capsular contracture by silicone breast implants: Possible causes, biocompatibility, and prophylactic strategies. *Med Devices (Auckl.)* 2013;6:211–218.
2. Handel N, Jensen JA, Black Q, Waisman JR, Silverstein MJ. The fate of breast implants: A critical analysis of complications and outcomes. *Plast Reconstr Surg.* 1995;96:1521–1533.
3. Danino AM, Basmacioglu P, Saito S, et al. Comparison of the capsular response to the Biocell RTV and Mentor 1600 Siltex breast implant surface texturing: A scanning electron microscopic study. *Plast Reconstr Surg.* 2001;108:2047–2052.
4. Asplund O, Gylbert L, Jurell G, Ward C. Textured or smooth implants for submuscular breast augmentation: A controlled study. *Plast Reconstr Surg.* 1996;97:1200–1206.
5. Barnsley GP, Sigurdson LJ, Barnsley SE. Textured surface breast implants in the prevention of capsular contracture among breast augmentation patients: A meta-analysis of randomized controlled trials. *Plast Reconstr Surg.* 2006;117:2182–2190.
6. Maxwell GP, Scheflan M, Spear S, Nava MB, Hedén P. Benefits and limitations of macrotextured breast implants and consensus recommendations for optimizing their effectiveness. *Aesthet Surg J.* 2014;34:876–881.
7. Jewell ML, Jewell JL. A comparison of outcomes involving highly cohesive, form-stable breast implants from two manufacturers in patients undergoing primary breast augmentation. *Aesthet Surg J.* 2010;30:51–65.
8. Maxwell GP, Van Natta BW, Bengtson BP, Murphy DK. Ten-year results from the Natrelle 410 anatomical form-stable silicone breast implant core study. *Aesthet Surg J.* 2015;35:145–155.
9. Brown MH, Shenker R, Silver SA. Cohesive silicone gel breast implants in aesthetic and reconstructive breast surgery. *Plast Reconstr Surg.* 2005;116:768–779; discussion 780–781.
10. Giot JP, Paek LS, Nizard N, et al. The double capsules in macro-textured breast implants. *Biomaterials* 2015;67:65–72.
11. Hall-Findlay EJ. Breast implant complication review: Double capsules and late seromas. *Plast Reconstr Surg.* 2011;127:56–66.
12. Spear SL, Rottman SJ, Glicksman C, Brown M, Al-Attar A. Late seromas after breast implants: Theory and practice. *Plast Reconstr Surg.* 2012;130:423–435.
13. Mazzocchi M, Dessy LA, Carlesimo B, Marchetti F, Scuderi N. Late seroma formation after breast surgery with textured silicone implants: A problem worth bearing in mind. *Plast Reconstr Surg.* 2010;125:176e–177e.
14. Rieger UM, Mesina J, Kalbermatten DF, et al. Bacterial biofilms and capsular contracture in patients with breast implants. *Br J Surg.* 2013;100:768–774.
15. Hu H, Jacombs A, Vickery K, Merten SL, Pennington DG, Deva AK. Chronic biofilm infection in breast implants is associated with an increased T-cell lymphocytic infiltrate: Implications for breast implant-associated lymphoma. *Plast Reconstr Surg.* 2015;135:319–329.
16. Loch-Wilkinson A, Beath K, Knight RJW, et al. Breast implant associated anaplastic large cell lymphoma in Australia and New Zealand: High surface area textured implants are associated with increased risk. *Plast Reconstr Surg.* 2017;140:645–654.
17. Abramo AC, De Oliveira VR, Ledo-Silva MC, De Oliveira EL. How texture-inducing contraction vectors affect the fibrous capsule shrinkage around breasts implants? *Aesthetic Plast Surg.* 2010;34:555–560.
18. Atlan M, Bigerelle M, Larreta-garde V, Hindié M, Hedén P. Characterization of breast implant surfaces, shapes, and biomechanics: A comparison of high cohesive anatomically shaped textured silicone, breast implants from three different manufacturers. *Aesthetic Plast Surg.* 2016;40:89–97.
19. Paek LS, Tétreault-Paquin JO, St-Jacques S, Nelea M, Danino MA. Is scanning electron microscopy a pertinent tool for the analysis of periprosthetic breast capsules? (in French). *Ann Chir Plast Esthet.* 2013;58:201–207.
20. Barr S, Hill E, Bayat A. Current implant surface technology: An examination of their nanostructure and their influence on fibroblast alignment and biocompatibility. *Eplasty* 2009;9:e22.
21. Danino A, Rocher F, Blanchet-Bardon C, Revol M, Servant JM. A scanning electron microscopy study of the surface of porous-textured breast implants and their capsules: Description of the "Velcro" effect of porous-textured breast prostheses (in French). *Ann Chir Plast Esthet.* 2001;46:23–30.
22. Lee KT, Mun GH. Updated evidence of acellular dermal matrix use for implant-based breast reconstruction: A meta-analysis. *Ann Surg Oncol.* 2016;23:600–610.
23. Yu D, Hanna KR, LeGallo RD, Drake DB. Comparison of histological characteristics of acellular dermal matrix capsules to surrounding breast capsules in acellular dermal matrix-assisted breast reconstruction. *Ann Plast Surg.* 2016;76:485–488.
24. van Heerden J, Turner M, Hoffmann D, Moolman J. Antimicrobial coating agents: Can biofilm formation on a breast implant be prevented? *J Plast Reconstr Aesthet Surg.* 2009;62:610–617.
25. Israeli R. Complications of acellular dermal matrices in breast surgery. *Plast Reconstr Surg.* 2012;130(Suppl 2):159S–172S.
26. Sbitany H, Serletti JM. Acellular dermis-assisted prosthetic breast reconstruction: A systematic and critical review of efficacy and associated morbidity. *Plast Reconstr Surg.* 2011;128:1162–1169.
27. Selber JC, Wren JH, Garvey PB, et al. Critical evaluation of risk factors and early complications in 564 consecutive two-stage implant-based breast reconstructions using acellular dermal matrix at a single center. *Plast Reconstr Surg.* 2015;136:10–20.
28. Hu H, Johani K, Almatroudi A, et al. Bacterial biofilm infection detected in breast implant-associated anaplastic large-cell lymphoma. *Plast Reconstr Surg.* 2016;137:1659–1669.
29. Constantine RS, Constantine FC, Rohrich RJ. The ever-changing role of biofilms in plastic surgery. *Plast Reconstr Surg.* 2014;133:865e–872e.
30. Chessa D, Ganau G, Spiga L, et al. *Staphylococcus aureus* and *Staphylococcus epidermidis* virulence strains as causative agents of persistent infections in breast implants. *PLoS One* 2016;11:e0146668.
31. Jordan SW, Khavanin N, Kim JY. Seroma in prosthetic breast reconstruction. *Plast Reconstr Surg.* 2016;137:1104–1116.
32. Ajdic D, Zoghbi Y, Gerth D, Panthaki ZJ, Thaller S. The relationship of bacterial biofilms and capsular contracture in breast implants. *Aesthet Surg J.* 2016;36:297–309.
33. Nyame TT, Lemon KP, Kolter R, Liao EC. High-throughput assay for bacterial adhesion on acellular dermal matrices and synthetic surgical materials. *Plast Reconstr Surg.* 2011;128:1061–1068.
34. Paek LS, Giot JP, Tétreault-Paquin JO, St-Jacques S, Nelea M, Danino MA. The impact of postoperative expansion initiation timing on breast expander capsular characteristics: A prospective combined clinical and scanning electron microscopy study. *Plast Reconstr Surg.* 2015;135:967–974.